Original Research Article

Structural Elucidation, 3D Molecular Modeling and Antibacterial Activity of Ni(II), Co(II), Cu(II) and Mn(II) Complexes

ABSTRACT

The ligand and its complexes of Ni(II), Co(II), Cu(II), and Mn(II) are explored in terms of synthesis, conductivity; magnetic measurements, elemental analysis, FT-IR; electronic spectra, and antibacterial activities. The 3D molecular modeling structures of the ligand and its metal complexes are obtained by using Argus lab software. The experimental data shows that the ligand is tetradentate and bonded to the metal ion *via* N_2O_2 donor atoms. Antibcterial activity of the synthesized compounds are checked against the microbes *Bacillus cereus* and *Escherichia coli.* The metal complexes exhibit antibacterial activity higher than that of the free ligand. This works contributes to the science of Schiff base compounds, in addition to stimulating the synthesis of new ligands and its complexes for the future advancement of coordination chemistry.

Keywords: *Schiff base; Tetradentate ligand; Complexation; Molecular modeling; Antibacterial activity*

1. INTRODUCTION

Schiff bases are considered as a very important class of compounds in organic chemistry. These are suitable candidates for the formation of coordination compounds with several metal ions *via* azomethine and phenolic groups. The general structural feature of Schiff base and its compounds is the azomethine group with a formula $RHC=NR_1$ where R and R_1 are alkyl, aryl, heterocyclic or cyclo alkyl groups which can be variously substituted.

Azomethine (C=N) linkage in the compounds is very important for biological activity, numerous azomethine derivatives has been reported to have notable antifungal, anticancer and antibacterial activities [1-3]. Therefore, they have attracted great attention of the scientists for the synthesis of metal complexes with Schiff bases and also for their easy formation and strong metal binding ability [4].

Schiff base ligands and its complexes can be employed for metal biosite modelling, nonlinear optical materials, model of reaction centres of metalloenzymes and luminescence materials [5, 6]. More importantly, Schiff base compounds have also played a vital role in the development of coordination chemistry [7, 8].

Metal complexes involving derivatives of salicylaldehyde and aromatic or aliphatic amines are of massive significance because of their potential use as catalyst for some catalytic reactions [9-13] and biological activities [14-16] etc. Salophen ligand offers a tetradentate chelating system to form stable metal complexes and thus they have very strong $\pi \rightarrow \pi^*$ intermolecular interactions. Metal complexes of salophen-type ligands have widespread applications as heterogeneous and homogeneous catalysts in many organic transformation reactions [17].

The 3D molecular modeling of compounds provides a three-dimensional image which permits a chemist to better see the manner in which atoms and molecules can interact. These models can be utilized to interpret existing observations or to predict new chemical behavior of the compounds.

With this background, the present work deals with the synthesis and characterization of salophen ligand and its complexes with Ni (II), Co (II), Cu (II), and Mn (II). The geometry of the synthesized compounds were confirmed by energy optimization through molecular mechanics calculation supported in Argus Lab software program. The antibacterial activity of the synthesized compounds were also examined herein.

2. MATERIALS AND METHODS

2.1 Reagents

All the starting reagents and materials used in this work were of standard analytical grade from Merck and Loba and used without further purification. Melting points were measured on a digital melting point apparatus. Elemental analyses for CHN were performed using a Vario EL cube [Germany elements (Elemental) analysis system]. UV-vis spectra were obtained on UV-Visible spectrophotometer [JASCO 503] using a quartz cuvette. FT-IR spectra were recorded on a FT-IR spectrophotometer [JASCO, FT-IR/4100] Japan using KBr pellets as the standard reference. ESI-MS spectra were done with an Agilent Technologies MSD SL Trap mass spectrometer with ESI source coupled with an 1100 Series HPLC system. Magnetic susceptibilities of the metal complexes were measured using a Sherwood Scientific MX Gouy magnetic susceptibility apparatus.

2.2 Synthesis of Schiff Base Ligand, L [$C_{20}H_{16}N_2O_2$]

To a stirring solution of *o*-Phenylenediamine (0.32g, 3 mmol) dissolved in about 20 mL ethanol, a solution of salicylaldehyde (0.64 mL, 6 mmol) in 10 mL of ethanol was added drop wise. This has resulted an orange color solution, which was refluxed for three hours (Scheme 1). The reaction mixture was cooled and kept for evaporation at room temperature leading to isolation of solid orange product. The product thus formed was filtered and washed several times with ethanol and dried in oven under 60^{o}C[18, 19]. The product was found to be soluble in DCM, DMF and DMSO.

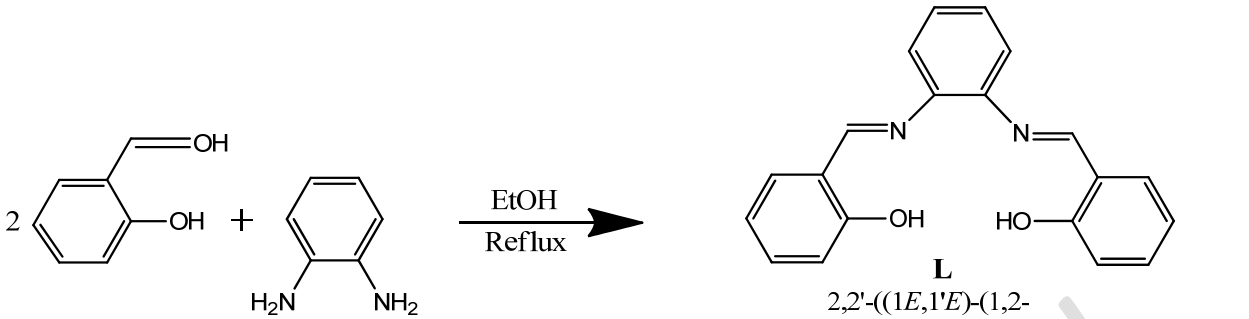

Scheme 1. Synthesis of Schiff base ligand, **L** [$C_{20}H_{16}N_2O_2$].

2.3 General Methods for the Synthesis of Metal Complexes

1 mmol of Schiff base ligand (L) dissolved in 10 mL ethanol was taken in a two necked round bottom flask and kept on magnetic stirring. After that, 1 mmol of metal salts (nickel acetate tetrahydrate for Ni-complex, cobalt acetate tetrahydrate for Co-complex, copper acetate monohydrate for Cu-complex and manganese chloride tetrahydrate for Mn-complex) dissolved in 20 mL of ethanol was added drop wise to the stirring solution. Then the reaction mixture was refluxed for about three hours. Aiming to remove the traces of unreacted starting materials, the complexes were then filtered and washed several times with ethanol and diethyl ether. Finally, the product was dried in oven under 60°C. It is important to note that all the synthesized complexes were soluble in DCM, DMF and DMSO. The proposed structure of the metal complex is illustrated in Fig. 1.

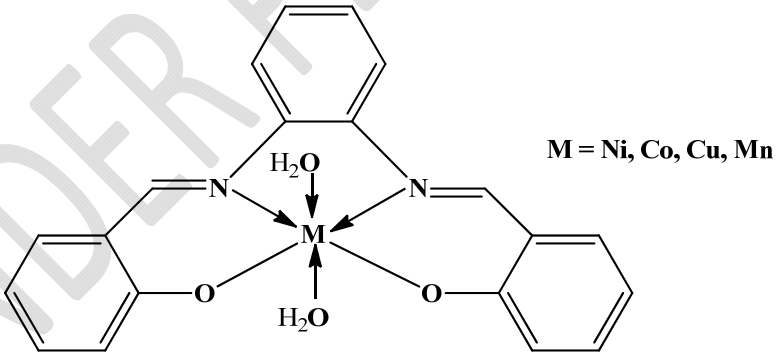

Fig. 1. Proposed structure of the synthesized complexes.

2.4 Metal Estimation

A known weight of the metal complex was taken into a conical flask and concentrated H_2SO_4 (500 μL) was added to it. It was fumed down to dryness and the process was repeated. Concentrated HNO_3 (500 μL) and $HClO_4$ (500 μL) were then added and the mixture was fumed to dryness. The process of adding acids and

fuming down to dryness was continued until there was no black materials. 100 mL distilled water was added to dissolve the residue. Finally, the metal was estimated complexometrically [20] and gravimetrically using EDTA (Ethylenediamine tetra acetic acid) and DMG (Dimethyl glyoxime). Excellent agreement of results were found.

2.5 Molecular Modeling Studies

The computational study of the synthesized compounds were done using molecular calculation with ArgusLab 4.0.1 version software.

2.6 Antibacterial Activity Study

Antibacterial activity was checked by the Agar-ditch method [21]. The *in vitro* antibacterial screening effects of the examined compounds were tested against *Bacillus cereus* and *Escherichia coli*. The compounds were dissolved in dimethyl sulfoxide (DMSO) to get final concentration of 5 $mgmL^{-1}$. In order to activate the bacterial strain, it was inoculated in 25 mL of Mac Conkey agar and incubated for 24 h at 37□C. Activated bacterial strain solution was prepared in normal saline (0.9% NaCl solution). The bacterial density was adjusted to 0.5 McFarland standard units. Mueller-Hinton agar was transferred over sterile 90 mm Petri dishes. Then 1 mL of activated bacterial strain solution was inoculated into the media at 40-45□C. The medium was permitted to solidify. Fine well was made with the help of cork borer in the plates and then the plates was filled with test solution (synthesized compounds dissolved in DMSO solution). Controls were run for the solvent and each bacteria. The plates were then incubated at 37□C for 24 h. The inhibition zones produced by the tested compounds were measured at the end of the incubation period.

3. RESULTS AND DISCUSSIONS

3.1 Synthesis

The Schiff base ligand, L was prepared in good yield from the condensation reaction of salicylaldehyde and *o*-phenylenediamine in a 2: 1 stoichiometric ratio. Treatment of the Ni(II), Co(II), Cu(II) and Mn(II) salts with the ligand L, formed complexes corresponding to 1:1 metal-ligand ratio. Physical and analytical data of studied compounds are presented in Table 1 and 2.

Table 1. Physical data of the ligand, L and its metal complexes.

Compound	Empirical Formula	FW (g/mol)	Colour (%yield)	m.p. (□C)
L	$C_{20}H_{16}N_2O_2$	316.35	Orange (83%)	190

NiL	$C_{20}H_{18}NiN_2O_4$	409.06	Red (78%)	>300
CoL	$C_{20}H_{18}CoN_2O_4$	409.30	Brown (84%)	>300
CuL	$C_{20}H_{18}CuN_2O_4$	413.91	Brown (80%)	>300
MnL	$C_{20}H_{18}MnN_2O_4$	405.31	Pink (82%)	>300

Table 2. Analytical data of the compounds.

Compound	Found (Calculated) (%)				μ_{eff} (B.M.)	Conductivity (μScm^{-1})
	M	C	H	N		
L	-	76.03 (75.93)	5.02 (5.10)	8.98 (8.86)	-	-
NiL	14.12 (14.35)	58.34 (58..72)	4.56 (4.44)	6.47 (6.85)	3.7	4
CoL	14.16 (14.40)	58.45 (58.69)	4.72 (4.43)	6.56 (6.84)	4.6	8
CuL	15.14 (15.35)	58.46 (58.03)	4.52 (4.38)	6.47 (6.77)	1.96	4
MnL	13.02 (13.55)	59.82 (59.27)	4.41 (4.48)	6.46 (6.91)	4.88	9

3.2 Molar Conductivity Measurements

The molar conductance values of 10^{-3} M solution of the metal complexes in DMSO are presented in Table 2. The low molar conductance value revealed that all the metal complexes were non-electrolyte in nature [22].

3.3 Elemental Analysis

The micro analysis data of the synthesized compounds are given in Table 2. The analytical data suggest that all the complexes are mononuclear. The data also reveal that metal to ligand ratio for the complexes is 1:1. Moreover, these data also supports the proposed structure of the ligand and complexes.

3.4 FT-IR Studies

FT-IR spectrum of the studied compounds are shown in Fig. 2-6. IR spectrum of the free ligand, L was compared with the spectra of the complexes to determine the binding mode of the ligand to metal in the complexes. Characteristic IR peaks of the ligand and its metal complexes are given in Table 3. From the IR spectrum it can be seen that, the diagnostic spectral bands of the ligand appeared at 1638 and 1298 cm^{-1} due to C=N and C–O vibrations, respectively. The characteristics azomethine stretching frequency at 1638 cm^{-1} of the free ligand was shifted to lower frequencies by some extent upon complexation suggesting coordination of Schiff base through azomethine nitrogen [23]. The strong band of phenolic C-O stretching vibration observed at 1298 cm^{-1} of the ligand was shifted towards lower frequencies on complexation, indicating phenolic oxygen atom

in Schiff base took part in complex formation [24]. The coordination through the azomethine nitrogen and phenolic oxygen to metal atom were further supported by the appearance of additional M-N & M-O vibrations in the region 761-753 cm^{-1} and 536 – 601 cm^{-1}, respectively in the IR spectra of metal complexes. The broad band appeared in the region 3434-3436 cm^{-1} together with new band in the region 631- 640 cm^{-1} in the spectra of the metal complexes confirmed the presence of coordinated water molecules. This suggests an octahedral geometry for all the complexes.

Table 3. IR (cm^{-1}), UV (nm) and ESI-MS data of the compounds.

Compound	*v* (O-H)	*v* (C=N)	v (C-O)	v (M-N)	v (M-O)	λ_{max}	ESI-MS
L	3467	1638	1298	-	-	272, 334	316.037
NiL	3436	1614	1277	761	581	264, 377, 478	409.004
CoL	3435	1620	1192	753	573	262, 309, 424	409.304
CuL	3434	1608	1187	754	536	263, 323, 420	413.087
MnL	3434	1623	1153	758	601	263, 331, 409	405.057

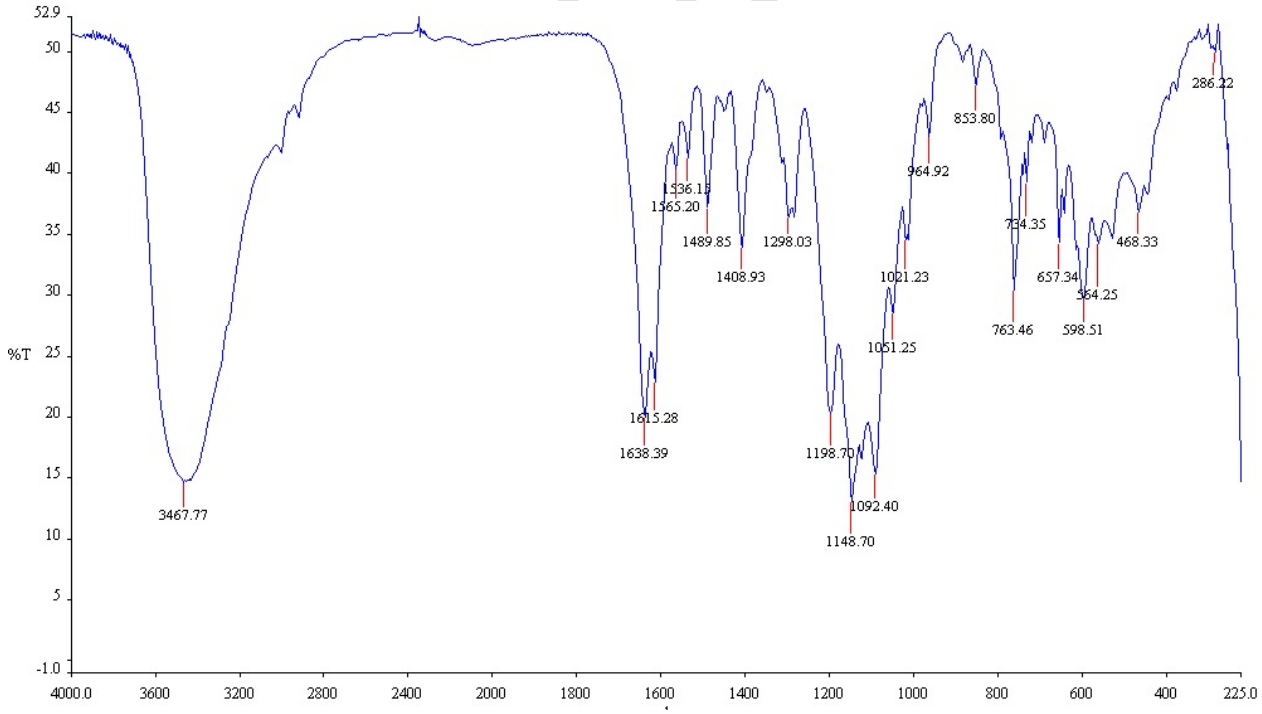

Fig. 2: IR spectrum of the ligand, L.

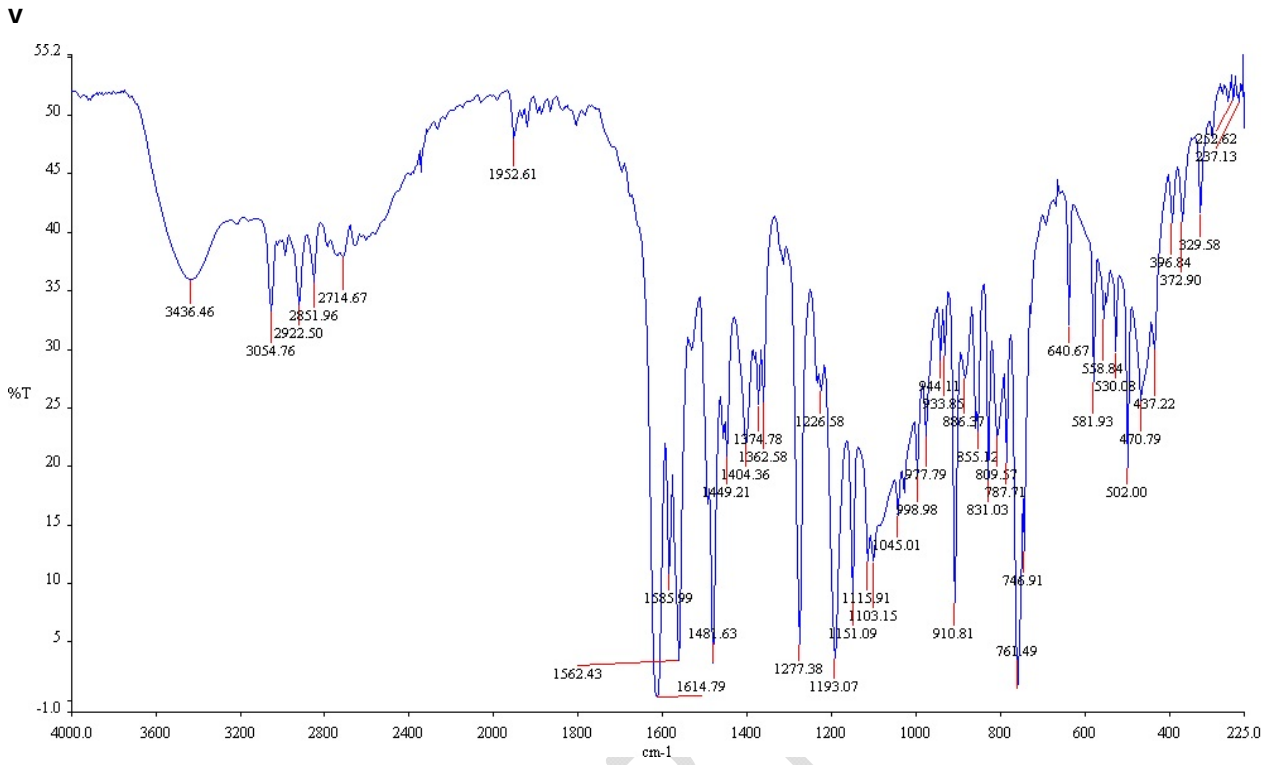

Fig. 3. IR spectrum of the complex, NiL.

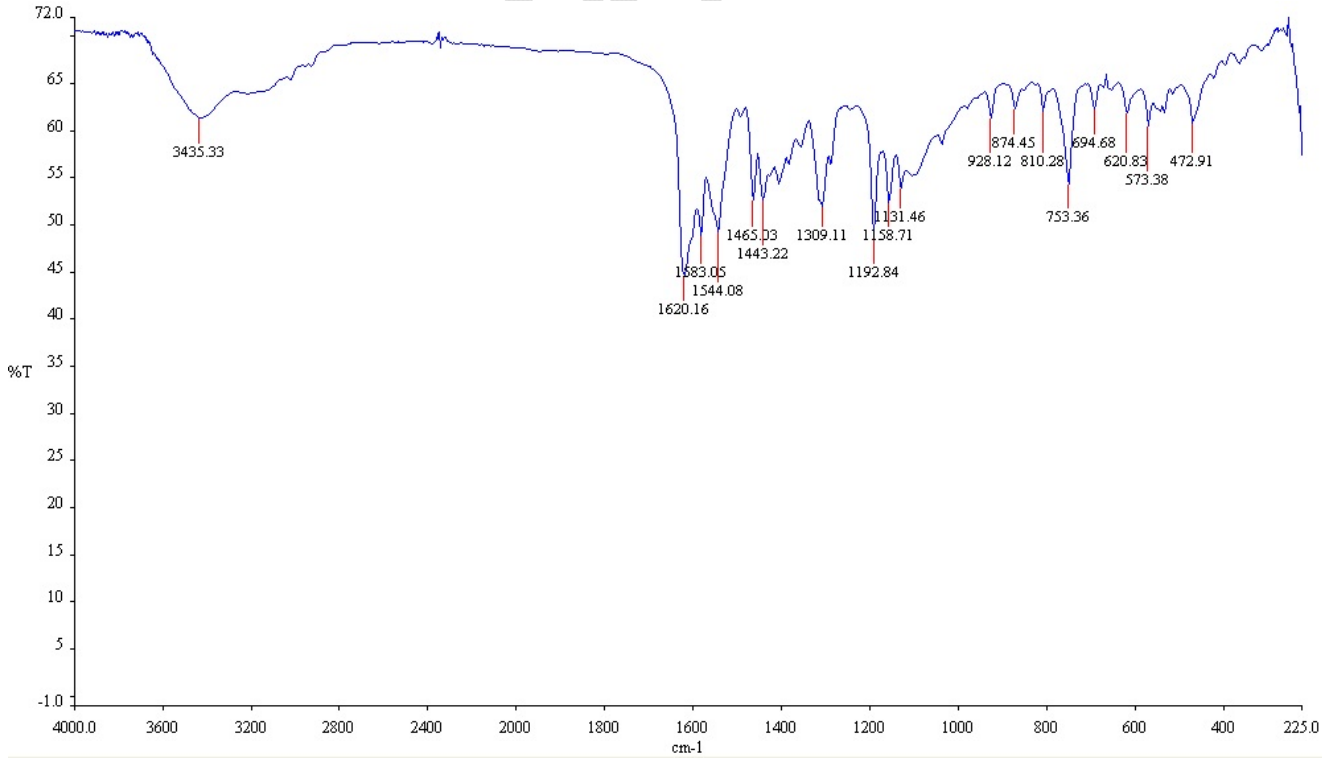

Fig. 4. IR spectrum of the complex, CoL.

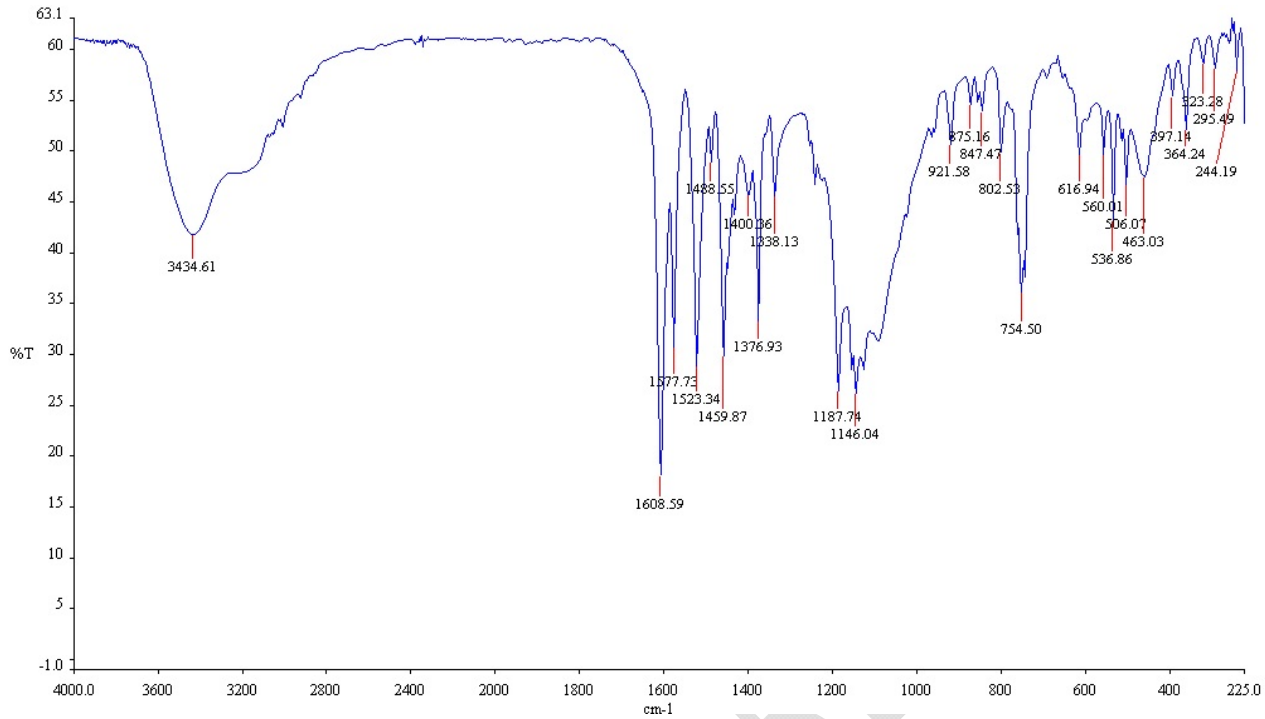

Fig. 5. IR spectrum of the complex, CuL.

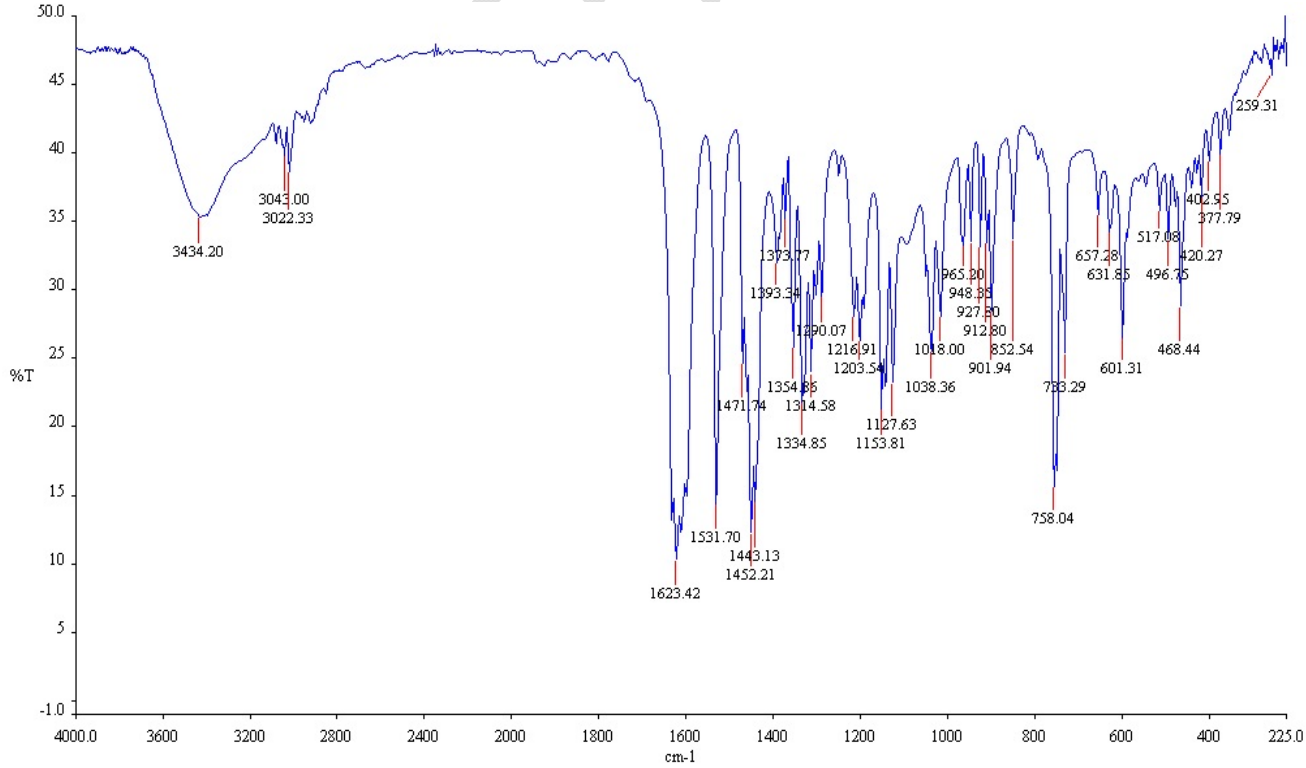

Fig. 6. IR spectrum of the complex, MnL.

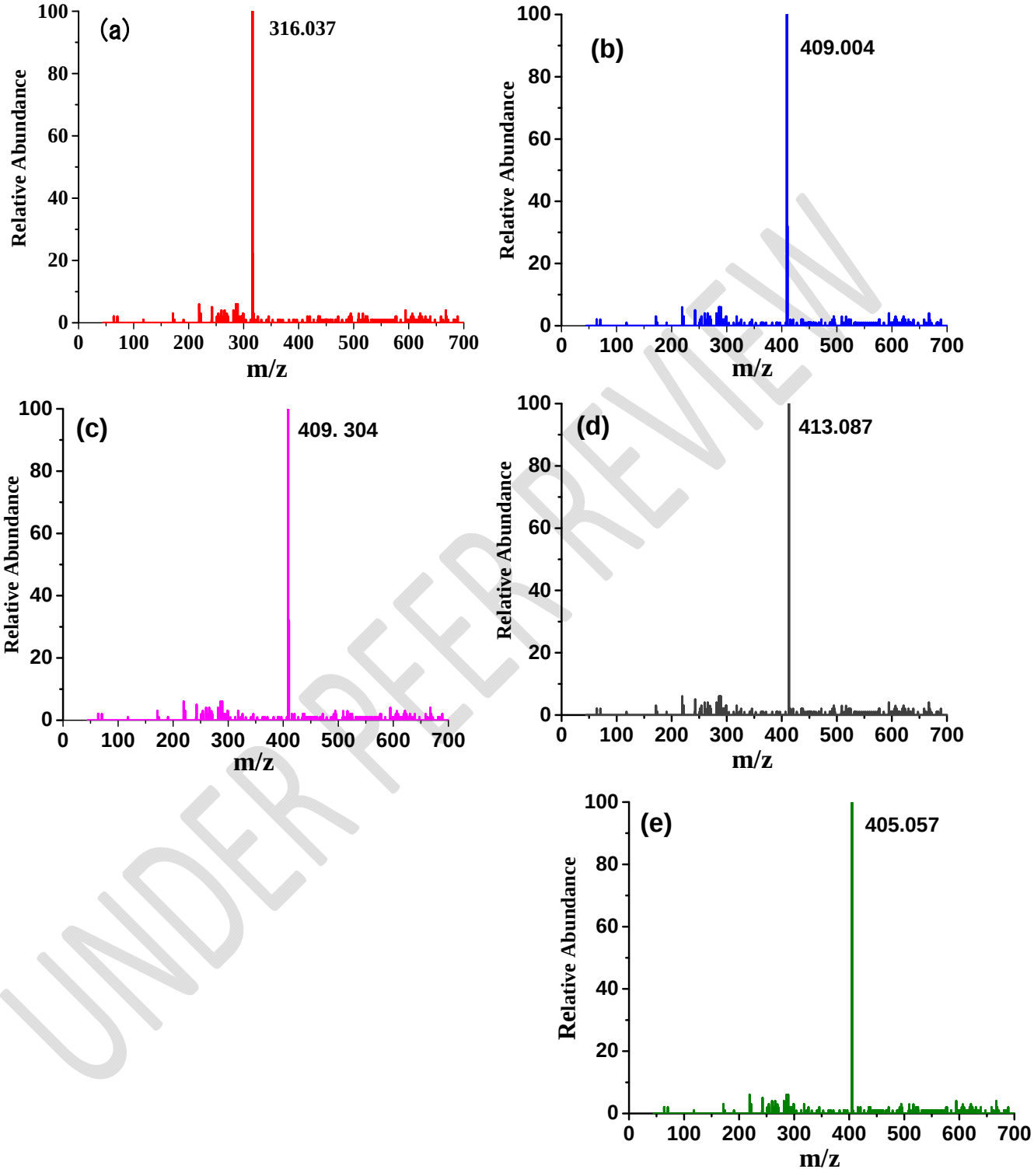

Fig. 7. ESI-Mass spectra of the (a) L, (b) NiL, (c) CoL, (d) CuL, and (e) M nL

3.5 ESI-Mass Spectra

The ESI-Mass spectra of the ligand and complexes are presented in Fig. 7. The obtained m/z values are similar to the formula weight (Table 3) which further supports the proposed structure of the synthesized compounds.

3.6 UV- visible Spectra and Magnetic Measurements

The electronic spectra of the ligand, L and all the complexes were recorded in DMSO at ambient temperature (Fig. 8). UV-visible spectral data are given in Table 3. The absorption band at 272 nm of the Schiff base ligand is due to benzene $\pi \rightarrow \pi^*$ transition [25]. Another band at 334 nm is attributed to the $n \rightarrow \pi^*$ transition of the non-bonding electron located on azomethine nitrogen atom of the ligand.

Usually, three different absorption bands are observed for an octahedral Ni(II) ion [26]. In this work, the electronic spectrum of the Ni(II) complex is well-matched with an octahedral geometry. Three absorption bands were observed for the Ni(II) complex at 264, 377 and 478 nm corresponding to the $^3T_{1g}(P) \rightarrow {}^3A_{2g}(F)$, $3T_{1g}(F) \rightarrow {}^3A_{2g}(F)$ and $^3T_{2g}(F) \rightarrow {}^3A_{2g}(F)$ transitions, respectively. On the basis of electronic spectral bands, an octahedral geometry is therefore proposed for the Ni(II) ion. The complex is paramagnetic with a magnetic moment of 3.7 B.M at room temperature.

In the UV-visible spectrum of the Co (II) complex, absorption peaks are observed around 262, 309, 424 nm regions due to $^4T_{1g}$ (F) $\rightarrow {}^4T_{1g}$ (P), $^4T_{1g}$ (F) $\rightarrow {}^4A_{2g}$ (P), and $^4T_{1g}$ (F) $\rightarrow {}^4T_{2g}$ (F), transitions respectively. The electronic spectral peak positions and high magnetic values (4.6 B.M) indicates an octahedral configuration for the complex CoL [26, 27].

The electronic spectra of the copper complex (CuL) show a band at 263 nm due to $^2B_{1g} \rightarrow {}^2E_g$ and two peaks at 323 and 420 nm assigned to d-d transitions and a charge transfer band, respectively, of an octahedral geometry [28, 29]. The hexa-coordinated Cu(II) ion with d^9 electronic configuration usually prefers distorted octahedral geometry, which is a direct consequence of Jahn–Teller effect [30]. Thus, octahedral complexes usually exist with a set of four strongly and two weakly coordinating ligands. Further confirmation was done by magnetic moment value 1.96 BM, which is consistent with proposed octahedral geometry of the complex, CuL [31, 32].

Mn (II) complexes display three bands 263, 331 and 409 nm assignable to $^4A_{1g}$ (4G) $\rightarrow {}^6A_{1g}$, $^4T_{2g} \rightarrow {}^6A_{1g}$ (4G) and $^4T_1g \rightarrow {}^6A_{1g}$ (G) transitions, which lie in the same range as reported for octahedrally coordinated Mn(II) ion [33]. The magnetic moment, 4.88 BM is an additional evidence for an octahedral structure.
From the electronic spectral and magnetic moment data of the synthesized compounds, it can be concluded that all of the metal complexes show an octahedral geometry in which ligands act as tetradentates.

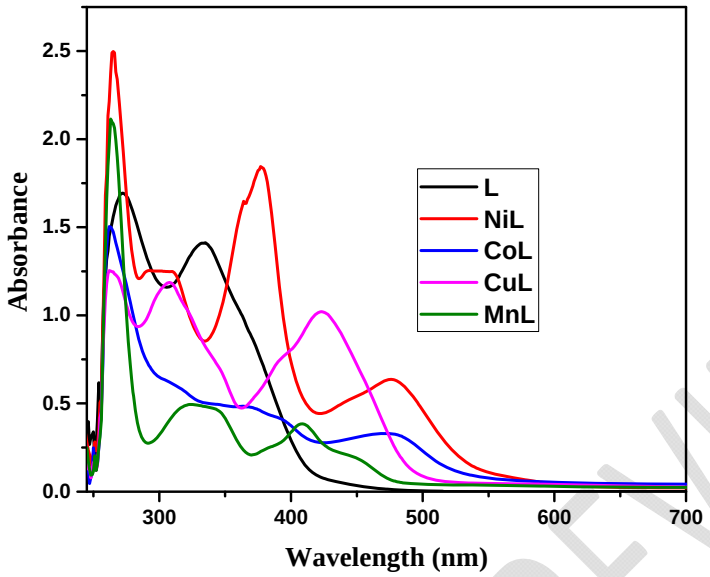

Fig. 8. Electronic spectra of the ligand and metal complexes.

3.7 Molecular Modeling Studies

The computational study of the compounds gives a clear idea about the three-dimensional arrangement of different atoms in the molecules. The probable geometry of the ligand, L and complexes were evaluated using molecular calculation with ArgusLab 4.0.1 version software [34, 35], presented in Fig. 9 and 10, respectively. The ligand structure was built and geometry optimization was performed using quantum mechanics based AM1 (Austin Model 1) approximation and also molecular orbital calculations were done. AM1 showed final self consistent field (SCF) energy, final geometrical energy and heat of formation for the synthesized ligand, -88203.1869, -88387.6244 and 47.7269 kcal/mol, respectively. After the geometry optimization by Universal Force Field (UFF) technique [36-38], the final geometrical energy of the ligand, L was 58.5771kcal/mol. The electron density surfaces of highest occupied molecular orbitals (HOMO) and lowest unoccupied molecular orbitals (LUMO) for the ground state of the synthesized ligand were obtained using AM1[Fig. 9 (b) and (c)]. On electrostatic potential (ESP) mapped electron density surface of L (Fig. 9(d)], red color shows the highest electron density region which is around phenolic O-atoms and mixed red and violet colors around azomethine N-atoms indicates the second highest electron density region. The high electron density around phenolic O- atoms and azomethine N-atoms is the reason for the coordination with metal ions and are in good support of the proposed structure of the complexes (Fig. 10). The 3D structure of the compounds is very significant in exploring the structure in the absence of XRD crystal structure data. The possible geometry for the Ni (II), Co (II), Cu (II), and Mn (II) complexes

were generated using molecular mechanics (UFF) calculations (Fig. 10). The details of the bonding and energy parameters optimized by molecular modeling calculations of the metal complexes are represented in Table 4.

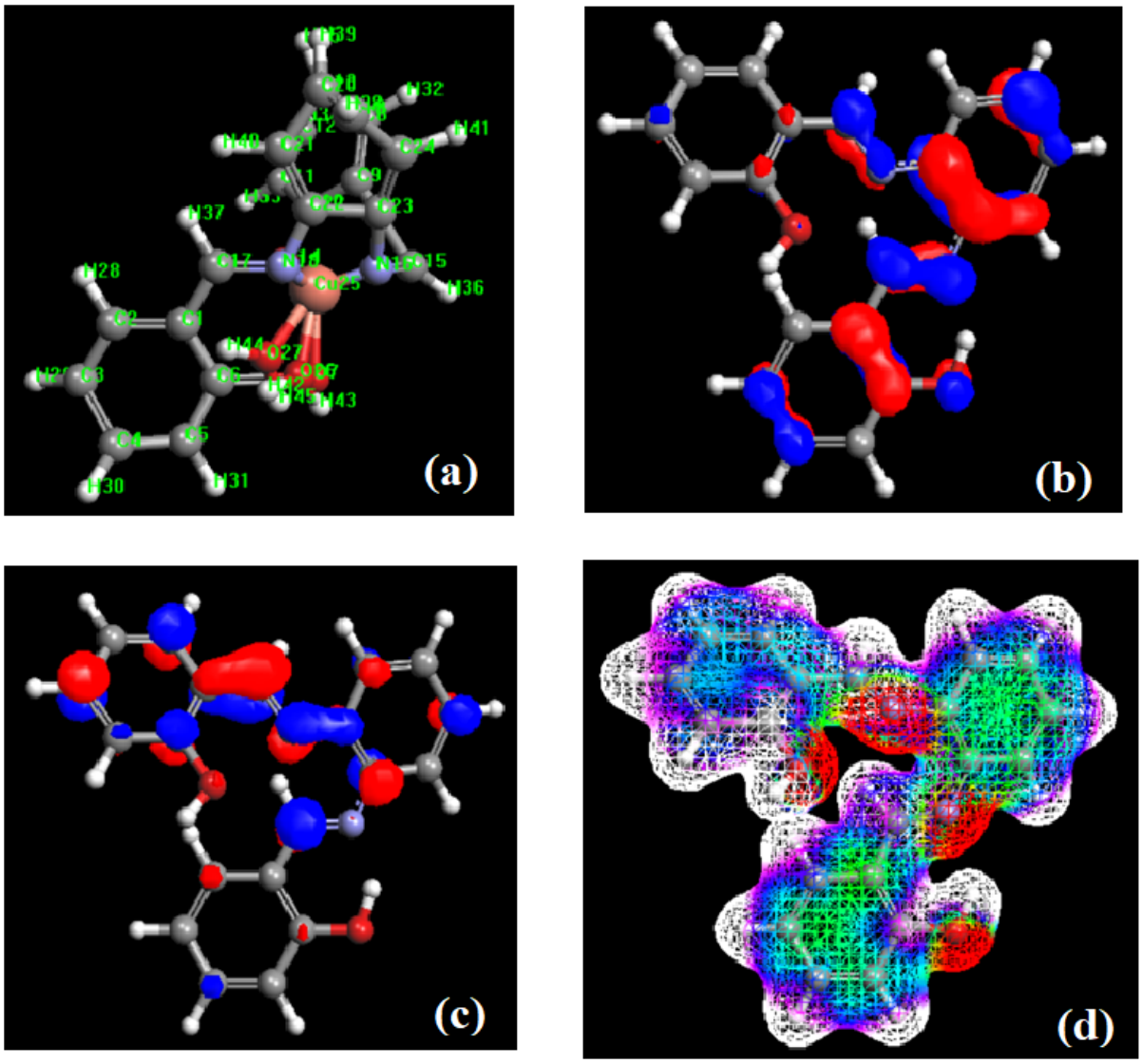

Fig. 9. Molecular modeling structure of the ligand, L, (a) optimized geometry, (b) HOMO, (c) LUMO and (d) Electrostatic potential mapped electron density surface.

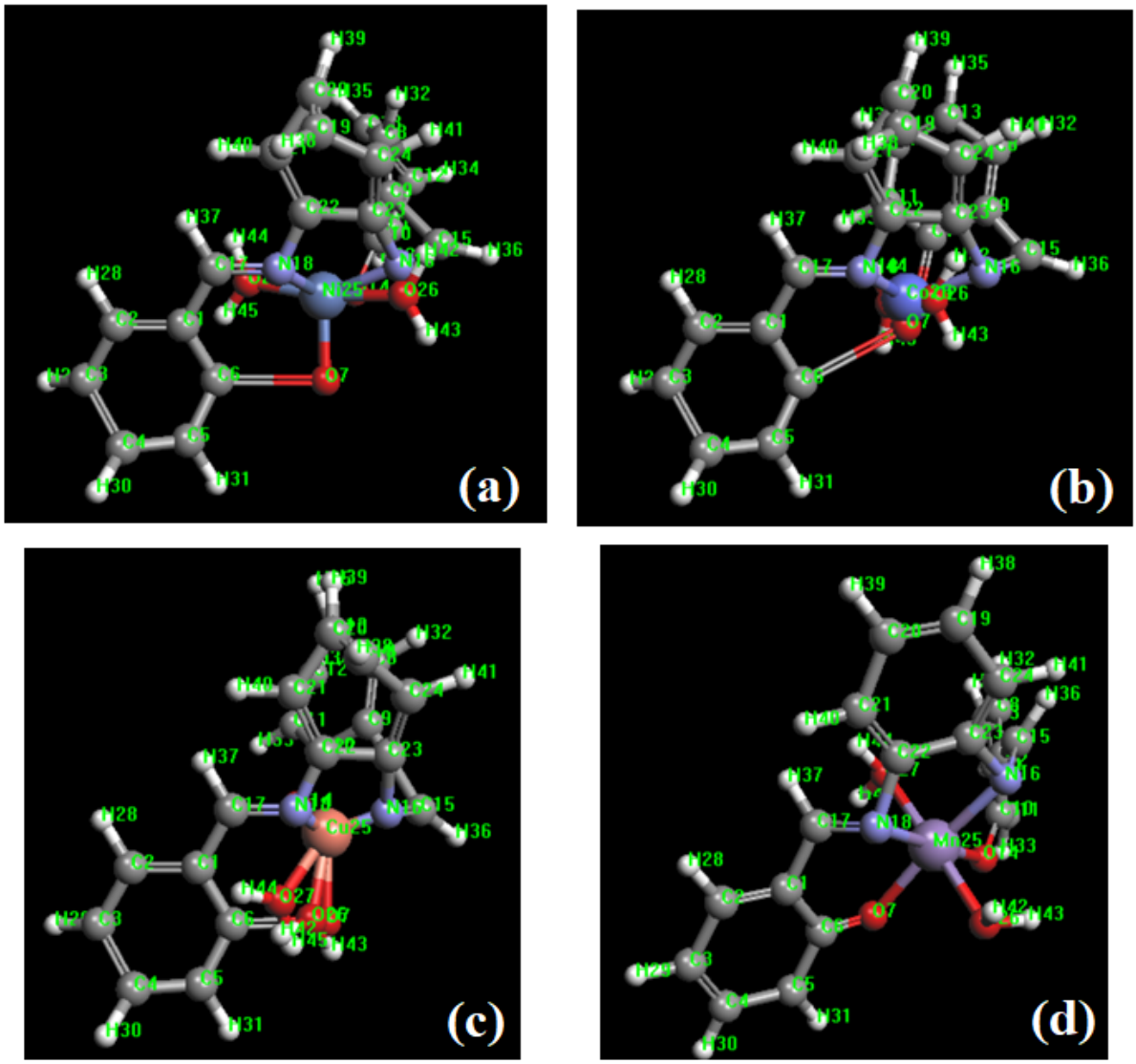

Fig. 10. Molecular modeling structure of the complexes, (a) NiL, (b) CoL, (c) CuL and (d) MnL.

Table 4. The selected bond lengths, bond angles and energy parameters of the complexes.

Complex	Atoms	Bond length (Angstrom)	Bond energy (kcal/mol)	Atoms	Bond angel (Degree)	Bond angel energy ((kcal/mol)	Final geometry energy ((kcal/mol)
NiL	O(7)-Ni(25) O(14)-Ni(25) N(16)-Ni(25) N(18)-Ni(25) Ni(25)-O(26) Ni(25)-O(27)	1.847 1.847 1.885 1.885 1.872 1.872	294.600 294.600 306.276 306.276 283.008 283.008	O(7)-Ni(25)-O(14) O(7)-Ni(25)-N(16) O(7)-Ni(25)-N(18) O(7)-Ni(25)-O(26) O(7)-Ni(25)-O(27) O(14)-Ni(25)-N(16) O(14)-Ni(25)-N(18) O(14)-Ni(25)-O(26) O(14)-Ni(25)-O(27) N(16)-Ni(25)-N(18) N(16)-Ni(25)-O(26) N(16)-Ni(25)-O(27) N(18)-Ni(25)-O(26) N(18)-Ni(25)-O(27) O(26)-Ni(25)-O(27)	90.00 90.00 90.00 90.00 90.00 90.00 90.00 90.00 90.00 90.00 90.00 90.00 90.00 90.00 90.00	295.751 316.977 316.977 289.809 289.809 316.977 316.977 289.809 289.809 340.090 310.824 310.824 310.824 310.824 284.114	124.7467
CoL	O(7)-Co(25) O(14)-Co(25) N(16)-Co(25) N(18)-Co(25) Co(25)-O(26) Co(25)-O(27)	1.939 1.939 1.972 1.972 1.939 1.939	254.562 254.562 267.453 267.453 254.562 254.562	O(7)-Co(25)-O(14) O(7)-Co(25)-N(16) O(7)-Co(25)-N(18) O(7)-Co(25)-O(26) O(7)-Co(25)-O(27) O(14)-Co(25)-N(16) O(14)-Co(25)-N(18) O(14)-Co(25)-O(26) O(14)-Co(25)-O(27) N(16)-Co(25)-N(18) N(16)-Co(25)-O(26) N(16)-Co(25)-O(27) N(18)-Co(25)-O(26) N(18)-Co(25)-O(27) O(26)-Co(25)-O(27)	90.00 90.00 90.00 90.00 90.00 90.00 90.00 90.00 90.00 90.00 90.00 90.00 90.00 90.00 90.00	255.557 275.391 275.391 255.557 255.557 275.391 275.391 255.557 255.557 296.982 275.391 275.391 275.391 275.391 255.557	254.0424

CuL	O(7)-Cu(25) O(14)-Cu(25) N(16)-Cu(25) N(18)-Cu(25) Cu(25)-O(26) Cu(25)-O(27)	1.997 1.997 2.016 2.031 2.022 2.022	168.223 168.223 181.007 176.938 162.029 162.029	O(7)-Cu(25)-O(14) O(7)-Cu(25)-N(16) O(7)-Cu(25)-N(18) O(7)-Cu(25)-O(26) O(7)-Cu(25)-O(27) O(14)-Cu(25)-N(16) O(14)-Cu(25)-N(18) O(14)-Cu(25)-O(26) O(14)-Cu(25)-O(27) N(16)-Cu(25)-N(18) N(16)-Cu(25)-O(26) N(16)-Cu(25)-O(27) N(18)-Cu(25)-O(26) N(18)-Cu(25)-O(27) O(26)-Cu(25)-O(27)	109.470 109.470 109.470 109.470 109.470 109.470 109.470 109.470 109.470 109.470 109.470 109.470 109.470 109.470 109.470	134.931 147.191 145.503 132.406 132.406 147.191 145.503 132.406 132.406 158.764 144.465 144.465 142.831 142.831 129.963	329.4080
MnL	O(7)-Mn(25) O(14)-Mn(25) N(16)-Mn(25) N(18)-Mn(25) Mn(25)-O(26) Mn(25)-O(27)	2.126 2.126 2.148 2.148 2.152 2.152	192.873 192.873 207.068 207.068 186.005 186.005	O(7)-Mn(25)-O(14) O(7)-Mn(25)-N(16) O(7)-Mn(25)-N(18) O(7)-Mn(25)-O(26) O(7)-Mn(25)-O(27) O(14)-Mn(25)-N(16) O(14)-Mn(25)-N(18) O(14)-Mn(25)-O(26) O(14)-Mn(25)-O(27) N(16)-Mn(25)-N(18) N(16)-Mn(25)-O(26) N(16)-Mn(25)-O(27) N(18)-Mn(25)-O(26) N(18)-Mn(25)-O(27) O(26)-Mn(25)-O(27)	90.00 90.00 90.00 90.00 90.00 90.00 90.00 90.00 90.00 90.00 90.00 90.00 90.00 90.00 90.00	193.626 210.973 210.973 190.113 190.113 210.973 210.973 190.113 190.113 229.930 207.206 207.206 207.206 207.206 186.731	102.9443

3.8 Antibacterial Activity

The antibacterial activity of the compounds were checked against the microorganism *Bacillus cereus* and *Escherichia coli*.

The compounds were investigated with a concentration of 5 $mgmL^{-1}$ employing agar ditch method. The zone of inhibition were measured in diameter (mm). The antibacterial activity results are presented in Table 5. All the metal complexes showed anti-bacterial activity over the free ligand. The ligand, L exhibited very little activity against both the organisms. The complex, CoL showed high activity against the microbes *Escherichia coli.* All other complexes exhibited almost similar activity. The variation in the activity of different metal complexes against tested organisms depends on either the impermeability of cells of organisms or the difference in ribosomes of bacterial cell [39]. The reasons of showing moderate to higher anti-bacterial activity of the complexes than that of free ligand can be explained on the basis of Overtone's concept and Tweedy's chelation model [40]. Polarity of metal ion is reduced to a greater extent due to the overlapping of the ligand orbital and partial sharing of positive

charge of metal ion with donor atoms of the ligand on chelation [41]. In addition, the delocalization of the π-electron is increased over the whole chelate sphere and improves the lipophilicity of the metal complex. The lipophilic character of the central metal atom is also increased upon chelation, which consequently favors the permeation through the lipid layer of cell membrane [42]. The variation in anti-bacterial activity is due to the cell membrane of the organisms and also the nature of metal ions.

Table 5. Antibacterial activity of the ligand L and its metal complexes (5 mg mL^{-1}).

Compound	Diameter of inhibition zone of bacteria (mm)	
	Gram positive	Gram negative
	Bacillus cereus	*Escherichia coli*
L	+	+
NiL	+ + +	+ + +
CoL	+ +	+ + +
CuL	+ + +	+ + +
MnL	+ +	+ +
DMSO	-	-

Control (DMSO): No activity (There was no inhibition zone)

Note: High activity = + + + (Inhibition zone > 12mm), Moderate = + + (Inhibition zone = 08-12mm) and Sight = + (Inhibition zone = 4-8 mm).

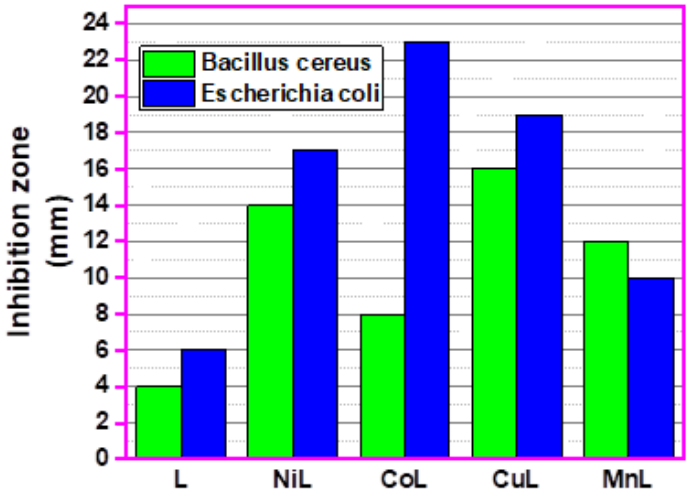

Fig. 11. Statistical representation for antibacterial activity for the ligand (L) and its complexes.

4. CONCLUSION

The spectral, elemental analysis, conductivity and magnetic measurements data, molecular modeling studies of the synthesized metal complexes of Ni(II), Co(II), Cu(II), and Mn(II) with the tetradentate ligand have shown octahedral geometry. The metal complexes are biological active and exhibit enhanced antibacterial activity compared to free ligand.

The antibacterial activity and chemical properties is dependent on molecular structure of the compound. Hence, substitution at the aromatic ring of the ligand and replacing coordinated water molecules to the central metal atom by unidentate N-, S-, or O-donor ligand can modify the electronic and steric properties of the resulting complexes, which can enable fine-tuning of chemical and biological properties of the ligands and metal complexes.

REFERENCES

1. Annapoorani, S. and C. Krishnan, *Synthesis and spectroscopic studies of trinuclear N4 Schiff base complexes international.* J. ChemTech Res, 2013. **5**(1): p. 180-185.
2. Mishra, A., R. Mishra, and M.D. Pandey, *Synthetic, spectral, structural and antimicrobial studies of some Schiff bases 3-d metal complexes.* Russian Journal of Inorganic Chemistry, 2011. **56**(11): p. 1757-1764.
3. Gunduzalp, A.B. and H.F. Ozbay, *The synthesis, characterization and antibacterial activities of dinuclear Ni (II), Cu (II) and Fe (III) Schiff base complexes.* Russian Journal of Inorganic Chemistry, 2012. **57**(2): p. 257-260.
4. Alaghaz, A.-N.M., et al., *Synthesis, spectroscopic identification, thermal, potentiometric and antibacterial activity studies of 4-amino-5-mercapto-S-triazole Schiff's base complexes.* Journal of Molecular Structure, 2015. **1087**: p. 60-67.
5. Keypour, H., et al., *Synthesis of two new N2O4 macroacyclic Schiff base ligands and their mononuclear complexes: Spectral, X-ray crystal structural, antibacterial and DNA cleavage activity.* Polyhedron, 2015. **97**: p. 75-82.
6. Borisova, N.E., M.D. Reshetova, and Y.A. Ustynyuk, *Metal-free methods in the synthesis of macrocyclic Schiff bases.* Chemical reviews, 2007. **107**(1): p. 46-79.
7. Mohammadi, K., S.S. Azad, and A. Amoozegar, *New tetradentate Schiff bases of 2-amino-3, 5-dibromobenzaldehyde with aliphatic diamines and their metal complexes: Synthesis, characterization and thermal stability.* Spectrochimica Acta Part A: Molecular and Biomolecular Spectroscopy, 2015. **146**: p. 221-227.
8. Dhahagani, K., et al., *Synthesis and spectral characterization of Schiff base complexes of Cu (II), Co (II), Zn (II) and VO (IV) containing 4-(4-aminophenyl) morpholine derivatives: Antimicrobial evaluation and anticancer studies.* Spectrochimica Acta Part A: Molecular and Biomolecular Spectroscopy, 2014. **117**: p. 87-94.
9. Isse, A.A., A. Gennaro, and E. Vianello, *Electrochemical carboxylation of arylmethyl chlorides catalysed by [Co (salen)][H 2 salen= N, N'-bis (salicylidene) ethane-1, 2-diamine].* Journal of the Chemical Society, Dalton Transactions, 1996(8): p. 1613-1618.
10. Nelson, S.G., T.J. Peelen, and Z. Wan, *Mechanistic alternatives in Lewis acid-catalyzed acyl halide aldehyde cyclocondensations.* Tetrahedron letters, 1999. **40**(36): p. 6541-6543.
11. Yoon, T.P., V.M. Dong, and D.W. MacMillan, *Development of a new Lewis acid-catalyzed Claisen rearrangement.* Journal of the American Chemical Society, 1999. **121**(41): p. 9726-9727.
12. Asraf, M.A., et al., *Cobalt salophen complexes for light-driven water oxidation.* Catalysis Science & Technology, 2016. **6**(12): p. 4271-4282.
13. Asraf, M.A., et al., *Earth-abundant metal complexes as catalysts for water oxidation; is it homogeneous or heterogeneous?* Catalysis Science & Technology, 2015. **5**(11): p. 4901-4925.

14. Tarafder, M., et al., *Coordination chemistry and bioactivity of some metal complexes containing two isomeric bidentate NS Schiff bases derived from S-benzyldithiocarbazate and the X-ray crystal structures of S-benzyl-β-N-(5-methyl-2-furylmethylene) dithiocarbazate and bis [S-benzyl-β-N-(2-furylmethylketone) dithiocarbazato] cadmium (II).* Polyhedron, 2002. **21**(27-28): p. 2691-2698.
15. Tarafder, M.T.H., et al., *Complexes of a tridentate ONS Schiff base. Synthesis and biological properties.* Transition Metal Chemistry, 2000. **25**(4): p. 456-460.
16. Patole, J., et al., *Schiff base conjugates of p-aminosalicylic acid as antimycobacterial agents.* Bioorganic & medicinal chemistry letters, 2006. **16**(6): p. 1514-1517.
17. Kocyigit, O., *Properties and Synthesis of the Cr (III)-Salen/Salophen Complexes Containing Triphenylamine Core.* Synthesis and Reactivity in Inorganic, Metal-Organic, and Nano-Metal Chemistry, 2012. **42**(2): p. 196-204.
18. Afsan, F., et al., *Synthesis, Spectral and Thermal Characterization of Selected Metal Complexes Containing Schiff Base Ligands with Antimicrobial Activities.* Asian Journal of Chemical Sciences, 2018: p. 1-19.
19. Mitu, L. and A. Kriza, *Synthesis and characterization of complexes of Mn (II), Co (II), Ni (II) and Cu (II) with an aroylhydrazone ligand.* Asian Journal of Chemistry, 2007. **19**(1): p. 658.
20. Schwarzenbach, G. and H.A. Flaschka, *Complexometric titrations [by] G. Schwarzenbach & H. Flaschka*. 1969, London: Methuen.
21. Parekh, J., et al., *Synthesis and antibacterial activity of some Schiff bases derived from 4-aminobenzoic acid.* JOURNAL-SERBIAN CHEMICAL SOCIETY, 2005. **70**(10): p. 1155.
22. Geary, W.J., *The use of conductivity measurements in organic solvents for the characterisation of coordination compounds.* Coordination Chemistry Reviews, 1971. **7**(1): p. 81-122.
23. Aranha, P.E., et al., *Synthesis, characterization, and spectroscopic studies of tetradentate Schiff base chromium (III) complexes.* Polyhedron, 2007. **26**(7): p. 1373-1382.
24. Abd-Elzaher, M.M., *Spectroscopic characterization of some tetradentate Schiff bases and their complexes with nickel, copper and zinc.* Journal of the Chinese Chemical Society, 2001. **48**(2): p. 153-158.
25. Temel, H. and S. Ilhan, *Synthesis and spectroscopic studies of novel transition metal complexes with schiff base synthesized from 1, 4-bis-(o-aminophenoxy) butane and salicyldehyde.* Russian journal of inorganic chemistry, 2009. **54**(4): p. 543-547.
26. Wade, K., *Ligand field theory and its applications, BN Figgis and MA Hitchman, Wiley–VCH, New York, 2000, xviii+ 354 pages.£ 51.95, ISBN 0.471-31776-4.* Applied Organometallic Chemistry, 2000. **14**(8): p. 449-450.
27. Lever, A.B.P., *Inorganic electronic spectroscopy.* 1968.
28. Haasnoot, J.G., *Mononuclear, oligonuclear and polynuclear metal coordination compounds with 1, 2, 4-triazole derivatives as ligands.* Coordination Chemistry Reviews, 2000. **200**: p. 131-185.
29. Alizadeh, M., F. Farzaneh, and M. Ghandi, *Heterogeneous catalysis in the liquid phase oxidation of alcohols by Cu (II) complexes immobilized between silicate layers of bentonite.* Journal of Molecular Catalysis A: Chemical, 2003. **194**(1-2): p. 283-287.
30. Reinen, D. and C. Friebel, *Copper (2+) in 5-coordination: a case of a second-order Jahn-Teller effect. 2. Pentachlorocuprate (3-) and other CuIIL5 complexes: trigonal bipyramid or square pyramid?* Inorganic Chemistry, 1984. **23**(7): p. 791-798.
31. Ruggiero, C.E., et al., *Synthesis and structural and spectroscopic characterization of mononuclear copper nitrosyl complexes: models for nitric oxide adducts of copper proteins and copper-exchanged zeolites.* Journal of the American Chemical Society, 1993. **115**(24): p. 11285-11298.
32. Willett, R.D., D. Gatteschi, and O. Kahn, *Magneto-structural correlations in exchange coupled systems.* 1985.

33. Jana, M.S., et al., *Octahedral Mn (II) complex with new NNO donor Schiff base ligand: Synthesis, structure, photoluminescent behavior and computational studies.* Polyhedron, 2014. **81**: p. 66-73.
34. Thompson, M., *MC Zerner œ A theoretical examination of the electronic structure and spectroscopy of the photosynthetic reaction center from rhodopseudomonas viridis œ J.* Am. Chem. Soc, 1991. **113**: p. 8210-8215.
35. Thompson, M.A., E.D. Glendening, and D. Feller, *The nature of K+/crown ether interactions: a hybrid quantum mechanical-molecular mechanical study.* The Journal of Physical Chemistry, 1994. **98**(41): p. 10465-10476.
36. Rappé, A.K., et al., *UFF, a full periodic table force field for molecular mechanics and molecular dynamics simulations.* Journal of the American chemical society, 1992. **114**(25): p. 10024-10035.
37. Casewit, C., K. Colwell, and A. Rappe, *Application of a universal force field to organic molecules.* Journal of the American chemical society, 1992. **114**(25): p. 10035-10046.
38. Rappe, A., K. Colwell, and C. Casewit, *Application of a universal force field to metal complexes.* Inorganic Chemistry, 1993. **32**(16): p. 3438-3450.
39. Mounika, K., A. Pragathi, and C. Gyanakumari, *Synthesis characterization and biological activity of a Schiff base derived from 3-ethoxy salicylaldehyde and 2-amino benzoic acid and its transition metal complexes.* Journal of Scientific Research, 2010. **2**(3): p. 513-513.
40. Tweedy, B., *Plant extracts with metal ions as potential antimicrobial agents.* Phytopathology, 1964. **55**: p. 910-914.
41. Thangadurai, T.D. and K. Natarajan, *Mixed ligand complexes of ruthenium (II) containing α, β-unsaturated-β-ketoaminesand their antibacterial activity.* Transition Metal Chemistry, 2001. **26**(4-5): p. 500-504.
42. Alias, M., H. Kassum, and C. Shakir, *Synthesis, physical characterization and biological evaluation of Schiff base M (II) complexes.* Journal of the Association of Arab Universities for Basic and Applied Sciences, 2014. **15**(1): p. 28-34.